

Fuzzy and Adaptive Control Strategies of Voltage Source Converter for Correction of Power Factor

V.NAVEEN¹, P. BHARAT KUMAR²

¹pg Student, Department Of EEE, JNTUA CEA, Anantapur, Andhrapradesh, India

²lecturer, Department Of EEE, JNTUA CEA, Anantapur, Andhrapradesh, India

Abstract—Due to the vast growth in semiconductor technology led to design of faster power electronic switches with higher ratings. These devices have been used to improve the performance of various power converter systems. To improve the power quality and power flow control the Voltage Source Converter (VSC) has been widely used in power systems. This work presents and compares the performance of three controllers namely vector control, Adaptive control and Fuzzy logic control schemes applied to a voltage source converter which operates an active power filter. The proposed method depends on an approximate third order nonlinear model of the VSC that accounts for the uncertainty in the three system parameters. The design ensures the asymptotic tracking of dc voltage and q -axis current reference trajectories. This approach is so-called full adaptive control. The design of Fuzzy control rule based on the general dynamic behaviour of the process. A new control method is implemented for suppressing the harmonics is fuzzy logic control. The power factor correction process is achieved without employing any complicated control logic. The performance of various controllers is examined and various simulations were carried out in MATLAB environment.

Key Words: Adaptive control, modelling, power factor correction, voltage source converter (VSC), fuzzy logic control.

1. INTRODUCTION

Voltage source converters (VSCs) have a number of important applications in the area of power conversion. They can be used as active power filters which compensate power factor of the supply or reject the harmonic content injected by a load. Both objectives have important consequences on the efficiency of the power supply. The proposed paper investigates the use

of model based adaptive and nonlinear control methods to achieve trajectory tracking for a number of power factor correction. The voltage source converter can provide bidirectional power flow, constant dc voltage and harmonic elimination. Voltage source converters have replaced complemented passive filters for number of power quality problems [1],[2] and [4]. This paper investigates the use of a VSC as a static synchronous compensator (STATCOM) to control power factor where the problem is to track VSC q -axis current and dc voltage. A number of approaches have been taken to solve this tracking problem. Some researchers exploit an approximate model, which assumes a time-scale separation between the voltage and current dynamics. For example, some approaches work in a synchronously rotating reference frame and use a decoupled proportional integral (PI) control for current and dc voltage [3], [10]. An improvement of vector control is proposed in [3] where additional PI controllers compensate undesired negative sequence components from an unbalanced load. The controller is designed based on a double synchronous reference frame. In order to facilitate controller tuning, improve transient, and steady-state performance, other approaches directly compensate for system nonlinearity. A PI control is cascaded with the d -axis current control to achieve robust tracking of constant dc voltage. The PI controller that improves decoupling of the d - and q -axes current dynamics. The technique is based on plant inversion. Since the multivariable PI control does not rely on feed forward control, system performance is robust to uncertainty. An optimization-based multivariable PI controller is proposed in [16]. The method is based on designing the nonparametric closed-loop and open-loop system matrices via convex optimization. The main objectives of the design are to provide fully decoupled d - and q -axes current dynamics and tracking performance with a simple structure. A stationary reference frame-based controller called proportional resonant (PR) controller provides an alternative to avoiding synchronous reference frame transformations. PR controllers can track time-varying reference trajectories with zero steady state error. Since the stationary frame

PR controllers essentially work like the PI controllers in the synchronous rotating frame, but without the need of frame transformations, they are likely to suffer from parameter robustness issues in a similar way to traditional vector control as in [3]. The control is designed without a synchronous reference frame transformation or current loop design. Adaptive control can be thought of as a feedback law that attempts to reshape the controller by observing its performance. This type of control is used to compensate for system uncertainty such as unknown parameters or disturbances [7]. In VSC applications, adaptive nonlinear control has been used to improve robustness to model error. A Lyapunov function-based adaptive back stepping control of a VSC, VSC is used as a rectifier feeding an unknown resistive load on the dc side. To reduce the complexity of the control design, the system uncertainties are assumed to be constant terms added to the VSC dynamics. The dc load current is also assumed constant. Model reference adaptive control (MRAC) was used for power factor correction in a second-order single-phase VSC with two unknown parameters [12]. In order to apply linear MRAC theory, a second-order nonlinear model is linearized around an equilibrium. Work in considers an adaptive control for two single-phase VSCs connected in parallel and having different output voltage levels. The controller is designed using a Lyapunov function and singular perturbation theories. A passivity based controller is proposed in that copes with unbalanced current and parameter uncertainties. The VSC model is developed using negative and positive sequence dynamics. Unlike the method proposed in this paper, none of the previous work involves an adaptive control for a third-order model with three unknown parameters. Hence, the proposed design accounts for a more precise VSC model and statements regarding its performance are improved in that regard. The other approach for VSC is fuzzy controller for power factor correction [13]. In [13], Voltage Source converter for the Improvement of Power Quality Using Fuzzy Logic Controller is described. The modelling of fuzzy logic controller is described in this paper. In [14], Presents a comparative evaluation of the proportional-integral, sliding mode and fuzzy logic controllers for applications to power converters and also demonstrates similarities of fuzzy logic controller with other controller. In [15], fuzzy logic controlled shunt active power filter for power quality improvement. This work presents improving power quality fuzzy logic controlled power filter.

2. VSC OPERATION AND MODELING

2.1 Basic Method of Operation

The VSC system shown in Fig. 1 Contains six IGBTs, each having an anti-parallel diode to provide a

path for current to flow it is off. Each leg of the converter has two IGBTs operating in complementary fashion, i.e., when the upper IGBT is off then the lower IGBT is in on state. The VSC is connected to a point of common coupling (PCC) to a three phase source and inductive load through filter inductors. The impedance of the each filter inductor, which also models IGBT conduction losses, is assumed balanced and equal to $R + j\omega L$, where ω is the ac source frequency. The voltages at PCC are denoted by v_a, v_b, v_c the currents flowing into the converters is i_a, i_b, i_c and the VSC terminal voltages are e_a, e_b, e_c . The VSC getting signals are g_1, g_2, \dots, g_6 are binary valued and generated by a Sinusoidal Pulse Width Modulation (SPWM) scheme.

2.2 Sinusoidal Pulse Width Modulation

The main objective of SPWM is to manipulate the low frequency components of the converter output voltage via high-frequency switching. Three-phase SPWM signals are generated based on comparing a triangle carrier waveform with three-phase modulation signals. The modulation signals are phase shifted by $2\pi/3$ rad and by δ relative to the ac source.

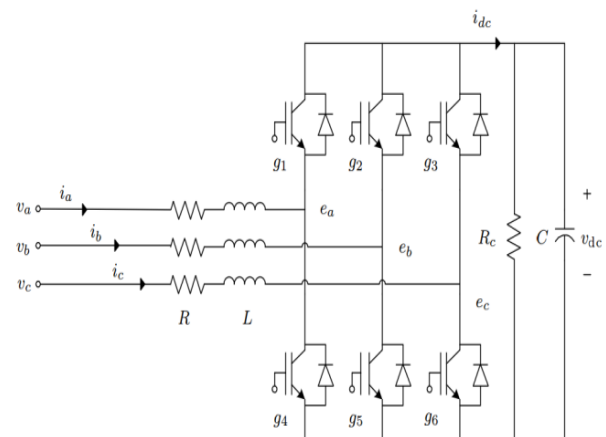


Fig-1: Circuit diagram of a VSC

Where δ is phase shift relative to the AC source. If the amplitude of the triangle carrier is A_c the ratio $m_a = A_m/A_c$ is known as an amplitude modulation index. It can influence the amplitude and phase of the fundamental components of the VSC output voltages by varying m_a and δ . In the SPWM for each phase is generated by comparing the three phase modulation signals with a carrier wave form. When the modulation signal is greater than the carrier waveform the SPWM output is high. When the modulation signal is lower than the carrier waveform the SPWM output is low.

2.3 VSC Modelling

Non Linear Model

The Fig. 3 shows typical shunt configurations of a VSC three-phase power system where the ac source currents are i_{sa}, i_{sb}, i_{sc} .

The VSC current dynamics can be written as

$$L \frac{di_a}{dt} + Ri_a = v_a - e_a$$

$$L \frac{di_b}{dt} + Ri_b = v_b - e_b$$

$$L \frac{di_c}{dt} + Ri_c = v_c - e_c$$

As in the power balance between the dc and ac sides of the VSC is

$$p - P_z = v_{dc}(\bar{i}_{dc}) \quad (2)$$

Where, 'p' is the instantaneous power into the VSC at the PCC and P_z is the instantaneous power dissipated in the impedance $R + j\omega L$ and \bar{i}_{dc} is the dc side current which related to dc voltage v_{dc} by

$$\bar{i}_{dc} - \frac{v_{dc}}{\bar{R}_c} = C \frac{dv_{dc}}{dt} \quad (3)$$

Where the capacitor resistance and switching losses are lumped into \bar{R}_c .

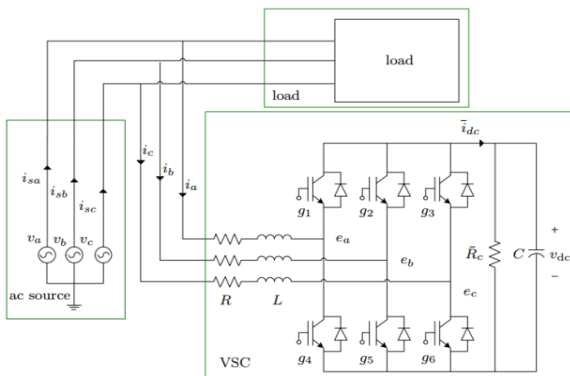


Fig-2: A typical shunt configuration of a VSC three-phase power system

From (1) and (2) we have

$$\frac{dv_{dc}}{dt} = \frac{p - P_z}{Cv_{dc}} - \frac{v_{dc}}{C\bar{R}_c} \quad (3)$$

The expressions for p and P_z are

$$p = v_a i_a + v_b i_b + v_c i_c$$

$$P_z = R(i_a^2 + i_b^2 + i_c^2) + L \left(i_a \frac{di_a}{dx} + i_b \frac{di_b}{dx} + i_c \frac{di_c}{dx} \right)$$

$$P_R = R(i_a^2 + i_b^2 + i_c^2)$$

$$P_L = L \left(i_a \frac{di_a}{dx} + i_b \frac{di_b}{dx} + i_c \frac{di_c}{dx} \right)$$

Where the P_R and P_L are resistance and inductor powers, respectively. The synchronously rotating reference frame transformation is used to express the system equations in dqo frame which is more convenient for control design [6]. We define the transformation which maps the phases from abc to dqo is given by

$$K(\omega t) = R(\omega t) \cdot S = \frac{2}{3} \begin{bmatrix} \sin(\omega t) & \cos(\omega t - \frac{2\pi}{3}) & \sin(\omega t + \frac{2\pi}{3}) \\ \cos(\omega t) & \sin(\omega t - \frac{2\pi}{3}) & \cos(\omega t + \frac{2\pi}{3}) \\ \frac{1}{2} & \frac{1}{2} & \frac{1}{2} \end{bmatrix}$$

This linear transformation is called the Clark Park Transformation or synchronous rotating reference frame transformation (RFT) matrix. The transformations are:

$$(i_d, i_q, i_0)^T = K \cdot (i_a, i_b, i_c)^T \text{ and}$$

$$(v_d, v_q, v_0)^T = K \cdot (v_a, v_b, v_c)^T$$

The ac supply is assumed balanced, the q-axis source voltage v_q can be considered zero. Therefore, the VSC system dynamics in dqo frame are

$$\begin{aligned} \frac{di_d}{dt} &= -\frac{R}{L} i_d + \omega i_q + \frac{v_d}{L} - \frac{e_d}{L} \\ \frac{di_q}{dt} &= -\frac{R}{L} i_q + \omega i_d + \frac{v_q}{L} - \frac{e_q}{L} \\ \frac{dv_{dc}}{dt} &= \frac{3}{2} \frac{v_d i_d + v_q i_q}{Cv_{dc}} - \frac{v_{dc}}{C\bar{R}_c} - \frac{P_z}{Cv_{dc}} \end{aligned} \quad (4)$$

Where v_d and v_q are d- and q-axis components of the ac source voltage. The VSC terminal voltages are denoted by e_d and e_q given by

$$e_d = \frac{1}{2} v_{dc} m_a \cos \delta \quad (5)$$

$$e_d = \frac{1}{2} v_{dc} m_a \cos \delta$$

These relations are derived from a time-average analysis of the VSC terminal voltage as a function of m_a and δ . Effectively, the amplitude and phase of the average value of the three-phase terminal voltages can be controlled through m_a and δ [5]. Since the fundamental component of the VSC terminal voltage has an amplitude of $v_{dc} m_a / 2$, the dc voltage must be controlled so that $v_{dc} > 2v_d$ to ensure proper VSC operation and bidirectional power flow. This paper considers a control design that allows for uncertainty in the parameters L, R, \bar{R}_c which are difficult to determine in practice.

Linear Model

The input $u = (u_1, u_2)^T$ is defined as $u_1 = (v_d - e_d), u_2 = (v_q - e_q)$

And the state as

$x = (x_1, x_2, x_3)^T = (i_d, i_q, \frac{C}{3v_d} v_{dc}^2)^T$ with the new choice of state and input dynamics (4) can be written as

$$\dot{x} = Ax + Bu + \Delta(x, u) \tag{6}$$

$$\bar{A} = \begin{bmatrix} -R/L & \omega & 0 \\ -\omega & -R/L & 0 \\ 1 & v_q/v_d & -2/(C\bar{R}_c) \end{bmatrix},$$

$$B = \begin{bmatrix} 1/L & 0 \\ 0 & 1/L \\ 0 & 0 \end{bmatrix}$$

$$\Delta(x, u) = [0 \quad 0 \quad -\frac{2P_z(x, u)}{3v_d}]^T \tag{7}$$

P_z can be expressed as a function of u

$$P_z(x, u) = P_R(x) + P_L(x, u) = \frac{3}{2} (u_1 i_d + u_2 i_q)$$

Since the VSC system is assumed balanced, it can be shown that P_L is negligible and P_R is almost constant. The effect of ac side resistor losses P_R can be included in the effective dc side resistance denoted \bar{R}_c . Then (1) and (3) can be replaced with

$$p = v_{dc} i_{dc} \tag{8}$$

And

$$\frac{dv_{dc}}{dt} = \frac{p}{C v_{dc}} - \frac{v_{dc}}{C \bar{R}_c} \tag{9}$$

Remove the over bar from R_c and i_{dc} in (9) to emphasize they can be different from \bar{R}_c and \bar{i}_{dc} as they related to a different VSC model.

After transforming (9) into dq frame, the VSC dynamics is

$$\dot{x} = Ax + Bu \tag{10}$$

$$A = \begin{bmatrix} -R/L & \omega & 0 \\ -\omega & -R/L & 0 \\ 1 & v_q/v_d & -2/(C R_c) \end{bmatrix}$$

Since we assume that P_L is negligible $P_z = P_R = \frac{3}{2} R(i_d^2 + i_q^2)$ therefore, we can express the relation between R_c and \bar{R}_c using

$$v_{dc}^2 \left(\frac{1}{C R_c} - \frac{1}{C \bar{R}_c} \right) = \frac{3}{2} R(i_d^2 + i_q^2) \tag{11}$$

Solve (22) for R_c gives

$$R_c = \left(1 + \frac{3R(i_d^2 + i_q^2)}{2v_{dc}^2} \bar{R}_c \right)^{-1} \bar{R}_c$$

$$= \frac{\bar{R}_c}{1 + P_R/P_{DC}} \tag{12}$$

Where the $P_{DC} = v_{dc}^2 / \bar{R}_c$ is the power loss of the resistance \bar{R}_c .

3. CLASSICAL VECTOR CONTROL OF A VSC

This is the traditional method of controller design for power quality improvement.

3.1 Classical Vector Control Of A VSC

In this classical vector control of a VSC is used for PFC. In this design assume all system parameters are known From (4),

Where R_c is used instead for simplicity, and defining e_d and e_q as

$$e_d = v_d + L(\omega i_q - p_1) \tag{13}$$

$$e_q = v_q + L(\omega i_d - p_2)$$

Where p_1 and p_2 are the outputs from the PI compensators of i_d and i_q .

Substituting the (13) into current dynamics in (1) gives decoupled equations

$$\frac{di_d}{dt} = -\frac{R}{L}i_d + p_1 \quad (14)$$

$$\frac{di_q}{dt} = -\frac{R}{L}i_q + p_2$$

By controlling i_d and i_q , consider the PI feedback

$$p_1 = K_{pd}(i_d^* - i_d) + K_{id} \int_0^1 (i_d^* - i_d) d\tau \quad (15)$$

$$p_2 = K_{pq}(i_q^* - i_q) + K_{iq} \int_0^1 (i_d^* - i_d) d\tau$$

Where $(.)^*$ denotes a desired reference value. In frequency domain we have

$$P_1(s) = \left(K_{pd} + \frac{K_{id}}{s} \right) (i_d^* - i_d)$$

$$P_2(s) = \left(K_{pq} + \frac{K_{iq}}{s} \right) (i_q^* - i_q) \quad (16)$$

From (14) and (15), closed-loop transfer functions of current dynamics are

$$\frac{I_d}{I_d^*} = \frac{K_{pd}s + K_{id}}{s^2 + (R/L + K_{pd})s + K_{id}} \quad (17)$$

$$\frac{I_q}{I_q^*} = \frac{K_{pq}s + K_{iq}}{s^2 + (R/L + K_{pq})s + K_{iq}} \quad (18)$$

The choice of parameters for the vector control gains is straight forward. Since (17) and (18) are second order linear transfer functions. Their outputs can't track time varying references. Therefore, i_d^* and i_q^* are considered to be constant, then the both two equations represent second order systems with un damped natural frequencies

$$\omega_{nd} = \sqrt{K_{id}} \quad \text{and} \quad \omega_{nq} = \sqrt{K_{iq}} \xi_d = (R/L + K_{pd}) / (2\sqrt{K_{id}}),$$

$$\xi_q = (R/L + K_{pq}) / (2\sqrt{K_{iq}}).$$

In some papers, filters are also used to cancel the closed-loop zeros. For PFC basic requirement is that i_q tracks the load reactive current i_{iq}^* . At the same time the controller should force v_{dc} to track constant reference v_{dc}^* . In designing the controller for the dc voltage dynamics, it is assumed that the dc voltage varies on slower time scale than the d-axis current. That is, when designing the control for dc voltage we assume i_d tracks its reference i_d^* . The dc voltage of the capacitor is related to the amount of real current entering the VSC,

dc voltage is indirectly controlled by d-axis current i_d . The output of the PI compensator for dc voltage is

$$I_d^*(s) = \left(k_{pv} + \frac{k_{iv}}{s} \right) (v_{dc}^* - V_{dc}) \quad (19)$$

The block diagram of the vector control is shown in Fig. 3. The dc voltage loops are taken as sufficiently lower in magnitude than those in the current loops. The PI gains for the dc voltage loop can be obtained from the transfer function of the dc voltage dynamics.

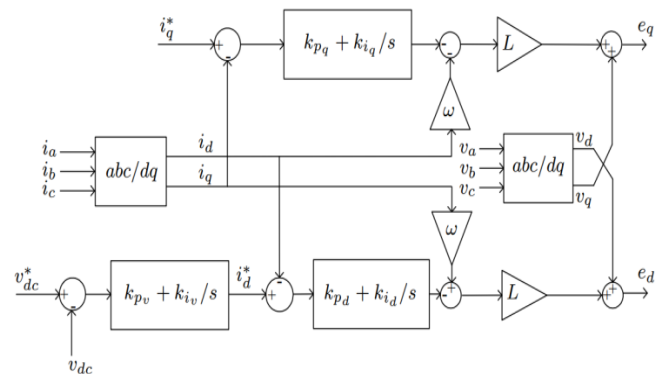


Fig-3: Block diagram of traditional vector control

4. FUZZY LOGIC CONTROLLER

Fuzzy Logic Controllers (FLCs) are designed based on the concept of fuzzy logic rule base. The advantage of fuzzy logic controllers over conventional controllers is they don't need an accurate mathematical model and they can handle non linearity, they can paper with number of imprecise inputs, and they are more robust than conventional controllers.

FLC consists of

1. Member ship values: member ship values we have to fuzzify the data or create membership values for the data and put them into fuzzy sets.
2. Rule table: the rule table must now be created to determine which output ranges are used. The table is an intersection of the two or more inputs.
3. Fuzzy rule base: fuzzy rules are writing based on rule table. After fuzzy rule base we get results then we de fuzzyfication using mamdani's method or any other method.

4.1 Fuzzy Logic Controller for VSC Compensation Principle

The active power filter is controlled to draw/supply the compensating current if from/to utility

to cancel out the current harmonics on AC side thereby making the source current in phase with source voltage thus improving the power factor.

Significance of DC Capacitor

The dc capacitor is present in the system, the dc capacitor has two main purposes: during steady state period it maintains DC voltage with small ripple and in the transient period it behaves as energy storage element to supply the real power difference between load and source. The load power changes there is a difference between load and source. When the load condition is changes there will be a disturbance in the real power balance between the load and source. Difference in the real power is compensated by DC capacitor voltage changes away from the reference voltage. For the satisfactory operation of the active filter, the peak value of the reference source current must be adjusted to proportionally change the real power drawn from the source. This real power charged/discharged by the capacitor compensates the real power consumed by the load. In DC capacitor voltage is recovered and reaches the reference voltage then, the real power supplied by the source is supposed to be equal to that consumed by the load again.

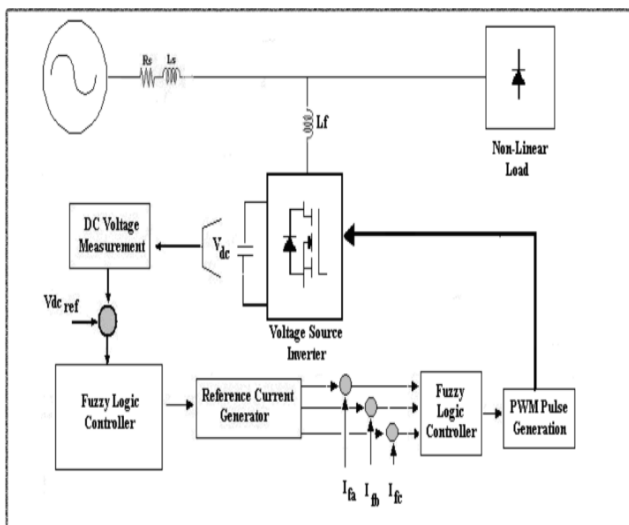


Fig-4: Basic Compensation Principle

It is in this way that, by regulating the average voltage of the DC capacitor the reference source current can be obtained.

4.2 Estimation of Reference Source Current

Ideal compensation demands the mains current to be sinusoidal and in phase with the source voltage, irrespective of the nature of load current. After

compensation, the desired source currents will be of the form.

$$I_{sa}^* = I_{sp} \sin \omega t$$

$$I_{sb}^* = I_{sp} \sin(\omega t - 120^\circ) \quad (20)$$

$$I_{sc}^* = I_{sp} \sin(\omega t + 120^\circ)$$

Where $I_{sp} = I_1 \cos \theta_1 + I_{SL}$ is the amplitude of the desired source current, while the phase angle can be obtained from the source voltages by multiply with the unit vectors of respective voltages, from Fig. 1, instantaneous currents can be written as

$$i_s(t) = i_L(t) - i_c(t) \quad (21)$$

Where $i_s(t), i_L(t), i_c(t)$ are instantaneous Source, filter and load currents respectively, source voltage is given by

$$V_s(t) = V_m \sin \omega t \quad (22)$$

Where $V_s(t), V_m$ are the instantaneous and peak values of source voltages respectively. If a non linear load is applied, to the load current can be represented as

$$i_L(t) = \sum_{n=1}^{\omega} I_n \sin(n\omega t + \phi_n) \quad (23)$$

$$i_L(t) = I_1 \sin(\omega t + \theta_1) + \sum_{n=2}^{\omega} I_n \sin(n\omega t + \phi_n)$$

The instantaneous load power can be given as

$$p_L(t) = V_s(t) * i_L(t)$$

$$p_L(t) = p_f(t) + p_r(t) + p_n(t) \quad (24)$$

The real power drawn by the load is given by

$$p_f(t) = V_m I_1 \sin^2 \omega t * \cos \theta_1$$

$$= V_s(t) * i_s(t) \quad (25)$$

From (25) the source current supplied by the source, after compensation is

$$i_s(t) = P_f(t) / V_s(t) = I_1 \cos \theta_1 \sin \omega t = I_{sm} \sin \omega t$$

Where $I_{sm} = I_1 \cos \theta_1$ there are also some switching losses in the PWM converter, and hence the utility must supply a small overhead for the capacitor leakage and converter switching losses in addition to the

real power of the load. The total peak current supplied by the source is therefore

$$I_{sp} = I_{sm} + I_{si} \quad (26)$$

Here we are considering the dc capacitor voltage for generation of error signal when compared with a reference value and actual source current is compared with reference source current in hysteresis controller to generate the switching signals. If the active filter provides the total harmonic power, then $i_s(t)$ will be in phase with the utility voltage and purely sinusoidal; At this instant, the active filter must be in a position to provide the following compensating current

$$i_c(t) = i_l(t) - i_s(t)$$

Hence, for accurate and instantaneous compensation of harmonic power it is necessary to estimate $i_s(t)$ which is the fundamental component of the load current as the reference current. Hence, the waveform and phase of the source currents are known and only their magnitudes are to be determined. This peak value of the reference current has been estimated by regulating the voltage of the DC capacitor of the PWM converter. The capacitor voltage is compared with a reference value and the error is proposed in a fuzzy logic controller. The output of the fuzzy controller is considered as the amplitude of the desired source current, and reference currents are estimated by multiplying this peak value with the unit sine vector in phase with the source voltages.

Estimation of Reference Current Template

Using the fuzzy logic controller, the peak value of reference current I_{max} is estimated by controlling the DC capacitor voltage in the closed loop. The output of the fuzzy control algorithm is the change in reference current $\delta I_{max}(n)$. The peak reference current at nth sampling time $I_{max}(n)$ is determined by adding the previous reference current $I_{max}(n-1)$ to the calculated change in reference current

$$I_{max}(n) = I_{max}(n-1) + \delta I_{max}(n) \quad (27)$$

This is an integrating effect which improves the steady state error in classical control theory.

6.3 Proposed Fuzzy Control Scheme

For implementing the control algorithm of a shunt active power filter in closed loop, the DC capacitor voltage is sensed and compared with a reference value. The obtained error

$$e(n) = V_{dc,ref}(n) - V_{dc,act}(n)$$

And changing error

$$Ce(n) = e(n) - e(n-1)$$

At the n^{th} sampling instants are taken as inputs for the fuzzy processing. After a limit, the output of the fuzzy controller is considered as the amplitude of the reference current I_{max} . This current I_{max} takes care of the losses in the system and the active power demand of load. By comparing the actual source currents (i_{sa}, i_{sb}, i_{sc}) with the reference current templates $(i_{sa}^*, i_{sb}^*, i_{sc}^*)$ in the hysteresis current controller, the switching signals for PWM converter are obtained. After proper amplification and isolation, the switching signals so obtained, are given to switches of the PWM converter.

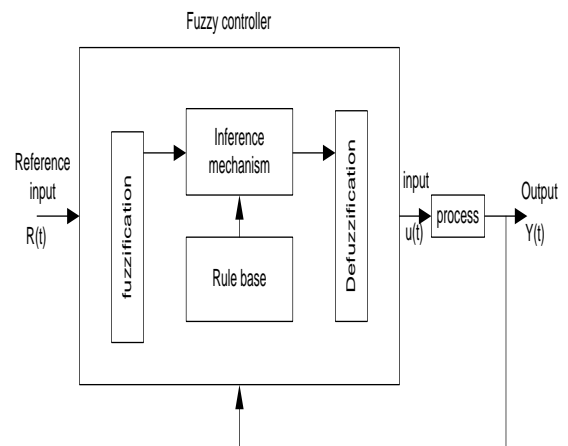


Fig-5: Block Diagram of Fuzzy Logic Controller

6.4 Basic Fuzzy Algorithm

The internal structure of the fuzzy controller is shown in Fig. 5. The error 'e' and change in error 'ce' are the real world numerical variables of the system. The FLC consists of three stages: the fuzzification, rule execution, and de fuzzification. In the first stage the crisp variables $e(k)$ and $de(k)$ are converted into fuzzy variables $E(k)$ and $dE(k)$ using the triangular membership functions shown in Fig. 6

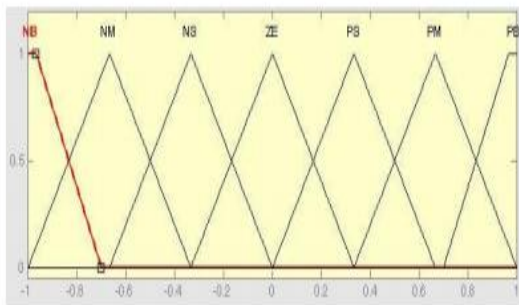


Fig-6(a): Input Membership Function

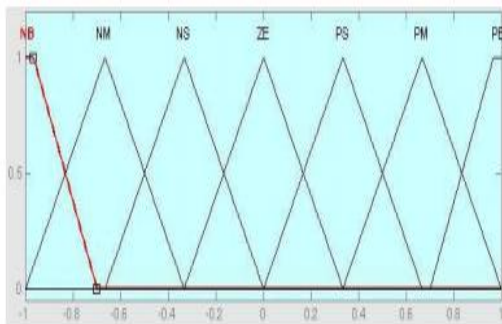


Fig-6 (b): Output Membership Function

Fig-6: Membership Function of the FLC

6.5 Rule Base

The elements of the rule base table are determined based on the theory that in the transient state, large errors need coarse control which requires coarse input/output variables and in the steady state, small errors need to fine control, which require fine input/output variables. Based on this the elements of the rule table are obtained as shown in Table. 1, with 'e', 'ce' as inputs.

Table 1: Rule Base for fuzzy logic controller

CE→ E↓	NB	NM	NS	ZE	PS	PM	PD
NB	NB	NB	NB	NB	NM	NS	ZE
NM	NB	NB	NB	NM	NS	ZE	PS
NS	NB	NB	NM	NS	ZE	PS	PM
ZE	NB	NM	NS	ZE	PS	PM	PB
PS	NM	NS	ZE	PS	PM	PB	PB
PM	NS	ZE	PS	PM	PB	PB	PB
PB	ZE	PS	PM	PB	PB	PB	PB

PWM Switching Law

The switching device is the PWM converter. The switching signals are obtained as: if $i_{sl} > V_{sl}$. The upper switch of the i^{th} leg is ON and lower switch is OFF. Consequently if the upper switch of the i^{th} leg is OFF $i_{sl} < i_{sl}^*$ the upper switch of the i^{th} leg is OFF and lower switch is ON.

5. ADAPTIVE CONTROL

An adaptive control can be thought as a feedback law attempts to reshape the controller by observing its performance. This type of control is usually proposed to compensate for some kinds of system uncertainty such as unknown parameters or disturbances

Adaptive Control of VSC for Power Factor Correction

In this paper two adaptive controllers are designed to provide PFC using a VSC. The proposed adaptive controls account for uncertainty in the VSC circuit parameters R, L and R_c .

Adaptive Control Design

Let us define none zero parameters $\theta_1 = L$, $\theta_2 = R$, and denote their estimates as $\hat{\theta}_i = \theta_i - \tilde{\theta}_i$, $i = 1, 2, 3$ with $\tilde{\theta} = \begin{pmatrix} \tilde{\theta}_1 & \tilde{\theta}_2 \\ \tilde{\theta}_1 & \tilde{\theta}_1 \end{pmatrix}^T$. The tracking error is denoted $\tilde{x} = (\tilde{x}_1, \tilde{x}_2, \tilde{x}_3)^T$ with $\tilde{x}_i = x_i - x_{ir}$ where x_{ir} stands for reference trajectory. With proper choice of VSC inputs i.e., $u_1(x, \hat{\theta}, t)$ and $u_2(x, \hat{\theta}, t)$ the tracking error dynamics have the form

$$\dot{\tilde{x}} = \Psi \tilde{x} + \Gamma^T(x, \hat{\theta}, t) \tilde{\theta} \quad (28)$$

$\Psi \in R^{2 \times 2}$ is a constant Hurwitz matrix; $\Gamma(x, \hat{\theta}, t) \in R^{3 \times 3}$ is a smooth function uniformly bounded in t. taking linearizing control

$$u_2 = -\alpha_2 \hat{\theta}_1 + x_2 \hat{\theta}_2 \quad (29)$$

Where $\alpha_2(x, t) = -\omega x_1 + k_2 \tilde{x}_2 - \dot{x}_{2r}$ in which k_2 is a positive controller gain. substituting this control into the q-axis current dynamics gives

$$\dot{\tilde{x}}_2 = \alpha_2 \frac{\tilde{\theta}_1}{\theta_1} - k_2 \tilde{x}_2 + \frac{\tilde{\theta}_2}{\theta_1}$$

Where we have defined $\beta_2(x) = -x_2$. next, the dc voltage tracking error dynamics are considered and can be used to define a reference for the d-axis current

$$\dot{x}_3 = (\dot{x}_1 + x_{1r}) + \frac{v_q}{v_d} x_2 - \frac{2\theta_3}{C} x_3 - \dot{x}_{3r}$$

Taking

$$x_{1r} = - \left(\frac{v_q}{v_d} x_2 + \gamma_3 \hat{\theta}_3 - \dot{x}_{3r} + k_3 (x_3 - x_{3r}) \right) \quad (30)$$

Where $\gamma_3 = -2x_3/C$, gives the tracking dynamics

$$\dot{x}_3 = -k_3 \tilde{x}_3 + \tilde{x}_1 + \gamma_3 \tilde{\theta}_3$$

Using (4.16) and the input

$$u_1 = -\alpha_1 \hat{\theta}_1 + x_1 \hat{\theta}_2 \quad (31)$$

We obtain the d-axis tracking error dynamics

$$\dot{x}_1 = -k_1 \tilde{x}_1 + \left(\alpha_1 + \frac{v_q}{v_d} \alpha_2 \right) \frac{\tilde{\theta}_1}{\theta_1} + \left(\beta_1 + \frac{v_q}{v_d} \beta_2 \right) \frac{\tilde{\theta}_2}{\theta_2} + \gamma_1 \tilde{\theta}_3$$

Where

$$\alpha_1 = \omega x_2 + \xi_3 (x_1 + \gamma_3 \hat{\theta}_3) + \gamma_3 \dot{\hat{\theta}}_3 - k_3 \dot{x}_{3r} - \dot{x}_{3r} + k_1 \tilde{x}_1 + \frac{v_q}{v_d} \left(-k_2 (x_2 - \dot{x}_{2r}) + \xi_3 x_2 + \dot{x}_{2r} \right) \lim_{t \rightarrow \infty} \int_0^t \tilde{x}^T(\tau) Q \tilde{x}(\tau) d\tau = V(0) - V(\infty) < \infty \quad (38)$$

$$\beta_1(x, t) = -x_1$$

$$\xi_3 = k_3 - \frac{2\hat{\theta}_3}{C}, \quad \gamma_1 = \varepsilon_3 \gamma_3$$

Hence, the error dynamics is in form (28) with

$$\Psi = \begin{bmatrix} -k_1 & 0 & 0 \\ 0 & -k_2 & 0 \\ 1 & 0 & -k_3 \end{bmatrix},$$

$$\Gamma = \begin{bmatrix} \alpha_1 + (v_q/v_d)\alpha_2 & \alpha_2 & 0 \\ \beta_1 + (v_q/v_d)\beta_2 & \beta_2 & 0 \\ \gamma_1 & 0 & \gamma_3 \end{bmatrix}$$

In order to analyze the convergence of the tracking error we consider the quadratic lyapunov function

$$V = \tilde{x}^T P \tilde{x} + \tilde{\theta}^T \Lambda^{-1} \tilde{\theta} \quad (32)$$

Where $\Lambda \in R^{2 \times 2}$ is a symmetric positive definite matrix and $P \in R^{2 \times 2}$ is the symmetric positive definite solution of

$$\Psi^T P + P \Psi = -Q \quad (33)$$

Where $Q \in R^{2 \times 2}$ is a symmetric positive definite matrix. Since Ψ is Hurwitz, there exists a unique symmetric positive definite matrix P which satisfies (33). The derivative of (32) along the error dynamics (28) is

$$\dot{V} = \tilde{x}^T (\Psi^T P + P \Psi) \tilde{x} + 2\tilde{x}^T P \Gamma^T \tilde{\theta} + 2\tilde{\theta}^T \Lambda^{-1} \tilde{\theta} \quad (34)$$

Hence taking parameter update law

$$\dot{\tilde{\theta}} = -\Lambda \Gamma P \tilde{x} \quad (35)$$

And substituting it into (34) yields

$$\dot{V} = -\tilde{x}^T Q \tilde{x} \leq 0 \quad (36)$$

Since V is positive definite and radially unbounded, the equilibrium $z = (\tilde{x}^T, \tilde{\theta}^T)^T = 0$ is globally uniformly stable and the solution $(\tilde{x}, \tilde{\theta})$ of (28) and (35) dynamics are uniformly bounded for any initial condition provided $v_{dc} > 2v_d$. Integration of (36) with respect to time gives

$$\int_0^t \tilde{x}^T(\tau) Q \tilde{x}(\tau) d\tau = - \int_0^t \dot{V}(\tau) d\tau = V(0) - V(\tau) \quad (37)$$

This implies

$$\lim_{t \rightarrow \infty} \int_0^t \tilde{x}^T(\tau) Q \tilde{x}(\tau) d\tau = V(0) - V(\infty) < \infty \quad (38)$$

Since z is bounded, according to Barbalat's Lemma we conclude $\lim_{t \rightarrow \infty} \|\tilde{x}\| = 0$ or the tracking error is asymptotically stable.

The conditions for parameter estimate error convergence follow from Matrosov's Theorem. A sufficient condition is given by

$$\Gamma(x_r, \tilde{\theta}, t)^T \Gamma(x_r, \tilde{\theta}, t) > 0$$

Although parameter error must remain bounded, convergence is not required to achieve asymptotic trajectory tracking.

In order to simplify the implementation of the parameter update law (35) we take Λ and P diagonal:

$$P = \begin{bmatrix} P_1 & 0 & 0 \\ 0 & P_2 & 0 \\ 0 & 0 & P_3 \end{bmatrix}, \Lambda = \begin{bmatrix} \Lambda_1 & 0 & 0 \\ 0 & \Lambda_2 & 0 \\ 0 & 0 & \Lambda_3 \end{bmatrix}$$

Where $P_i, \Lambda_i > 0, i = 1, 2$. This simple choice of P satisfies (33) for any Q .

Therefore, the parameter update law is

$$\dot{\tilde{\theta}}_1 = -\dot{\tilde{\theta}}_1 = \Lambda_1 \left(\left(\alpha_1 + \frac{v_q}{v_d} \alpha_2 \right) P_1 \tilde{x}_1 + \alpha_2 P_2 \tilde{x}_2 \right)$$

$$\dot{\tilde{\theta}}_2 = -\dot{\tilde{\theta}}_2 = \Lambda_2 \left(\left(\beta_1 + \frac{v_q}{v_d} \beta_2 \right) P_1 \tilde{x}_1 + \beta_2 P_2 \tilde{x}_2 \right) \quad (39)$$

$$\dot{\hat{\theta}}_3 = -\dot{\theta}_3 = \Lambda_3(\gamma_1 P_1 \hat{x}_1 + \gamma_2 P_2 \hat{x}_2)$$

We remark that the same technique and procedure can be used when the value for capacitance C is not known. In this case, the adaptive control would include an additional parameter. A block diagram of adaptive control system is shown in Fig. 7. From (28) and (39) there are nine gains Λ_i, P_i, k_i to be chosen which affect the transient closed-loop response. We establish approximate values for these gains based on a linearization of the closed-loop system (28) and (35) about an equilibrium point $z=0$:

$$\dot{z} = A_c z$$

Where

$$A_c = \begin{bmatrix} \Psi & A_{c12} \\ -\Lambda A_{c12}^T P & 0 \end{bmatrix}$$

$$A_{c12} = \begin{bmatrix} (1 - v_q/v_d)\omega x_{2r} & \gamma_{3r}\theta_3 & \xi_3\gamma_{3r} \\ (v_q/v_d)\omega x_{2r} + \omega\gamma_{3r}\theta_3 & -x_{2r} & 0 \\ 0 & 0 & \gamma_{3r} \end{bmatrix}$$

$$\xi_3 = k_3 - \frac{2\theta_3}{c}, \gamma_{3r} = -\frac{2x_{3r}}{c}$$

The characteristic polynomial of A_c can be used to obtain controller gains which approximately provide the desired transient performance. To account for nonlinearity, modelling errors, and disturbances we adjust the gains experimentally. The convergence rate of the parameter estimate and tracking error can be adjusted with Λ_i and k_i gains, respectively. This can be seen from the tracking error dynamics for zero parameter error, i.e., $\dot{x} = \Psi x$. Hence k_i directly controls the rate of convergence of \hat{x}_i and can be adjusted accordingly. The convergence rate for $\hat{\theta}_i$ can be adjusted with Λ_i with larger Λ_i providing faster convergence. It should be noted that larger values of P_i, Λ_i and k_i . Generally lead to larger amplitude control signals and faster transient performance. However, since the PWM modulation index m_a is bounded, transient response can be only so fast.

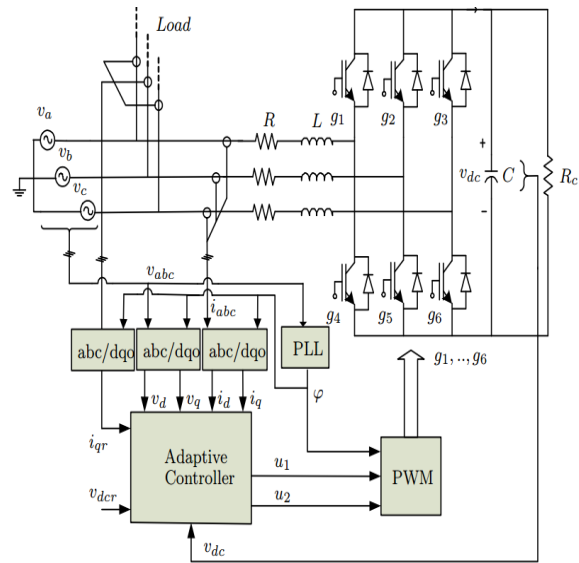


Fig-7: VSC adaptive control (ADC) block diagram

At each iteration first x_{1r} is computed using (23) which requires the VSC state, the reference q-axis current and dc voltage, and the parameter estimate $\hat{\theta}$. Next, the state reference x_r including calculated x_{1r} along with x and $\hat{\theta}$ give the control output u via (22) and (24). Finally, $\hat{\theta}$ is updated using (39). The parameter update is initialized as, $\hat{\theta}(0) = \hat{\theta}_0$.

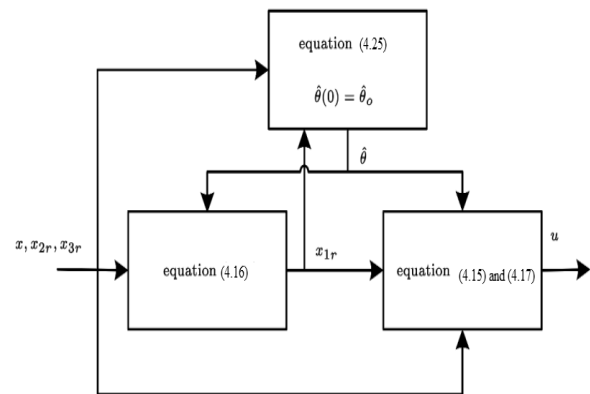


Fig-8: VSC adaptive control algorithm

6. SIMULATION RESULTS AND ANALYSIS

6.1 Traditional Vector Control

This section presents simulation results for the vector control applied to the nonlinear third order VSC model. The block diagram of control block is shown in Fig. 3. The control is applied to the third order nonlinear model and the nonlinear switched model of the VSC based on and Simulink SimPower system library.. Vector control gains are shown in Table 2 for traditional vector control.

TABLE 2: Vector Controller Gains

S.No	Gains	Value
1	(k_{dp}, k_{di})	(2 V/A, 100 V/(A.s))
2	(k_{qp}, k_{qi})	(4000 V/A, 30000 V/(A.s))
3	(k_{vp}, k_{vi})	(1 A/V, 5 A/(V.s))

TABLE 3: Nominal parameters used in simulation

S.No	Parameter	Value
1	L	2 mH
2	C	1100 μF
3	R	0.21 Ω
4	R_c	1.45 k Ω
5	ω	120 π rad/s
6	T	100 μs
7	v_d	60 V
8	v_q	0 V

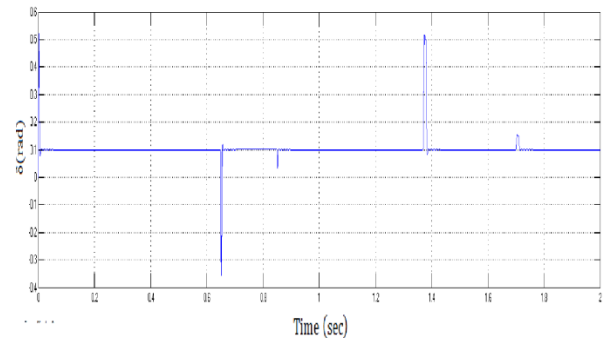
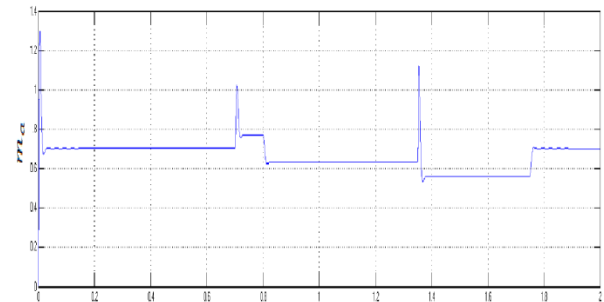
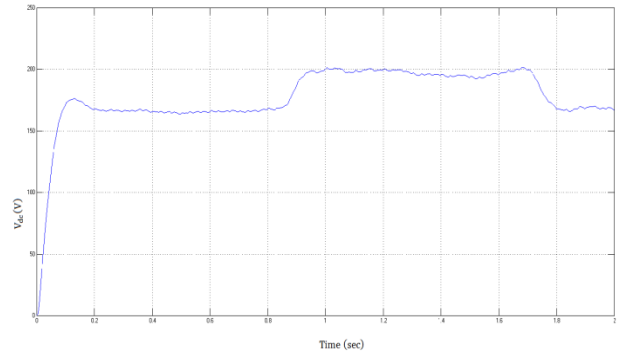
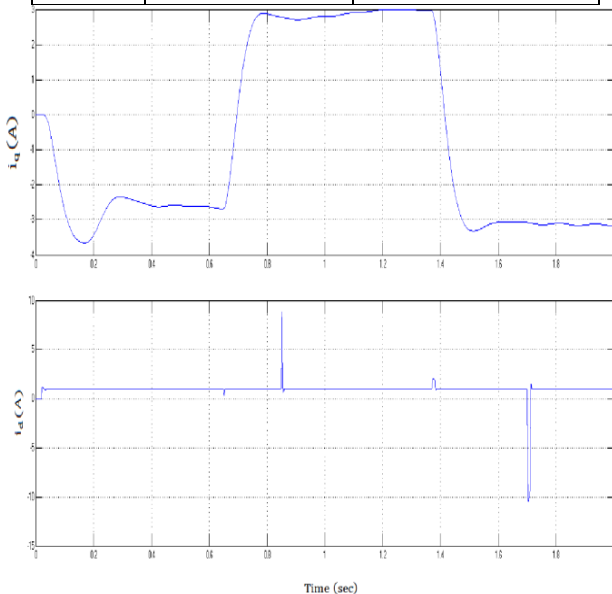


Fig 9 (a): Trajectories of voltage and currents

Fig-9 (b): Control inputs m_d and δ Figure.

Simulation results of vector control using the VSC nonlinear average model as shown in Fig. 9, the controller achieves good reference tracking and control inputs remain unsaturated. Performing vector control ωi_q and $-\omega i_d$ are canceled in i_d and i_q dynamics, this cancelation can only be performed exactly if L is known. Any deviation of L from its nominal value affects control performance. To investigate the effect of uncertainty in L, we take its value as half the nominal inductance.

6.2 Fuzzy logic Controller

The Simulation results of VSC with fuzzy logic controller for power quality improvement are shown in below Fig. 10.

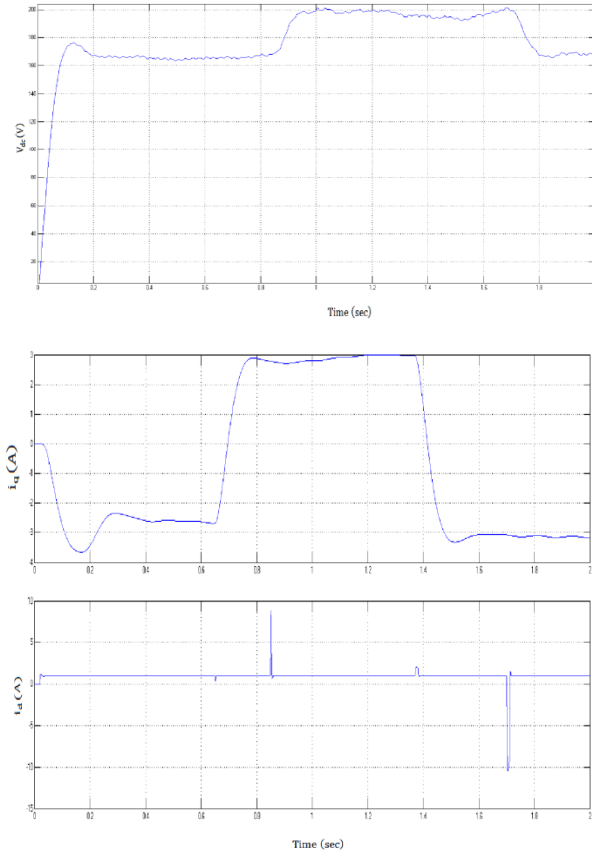


Fig-10 (a): Trajectories of voltage and currents.

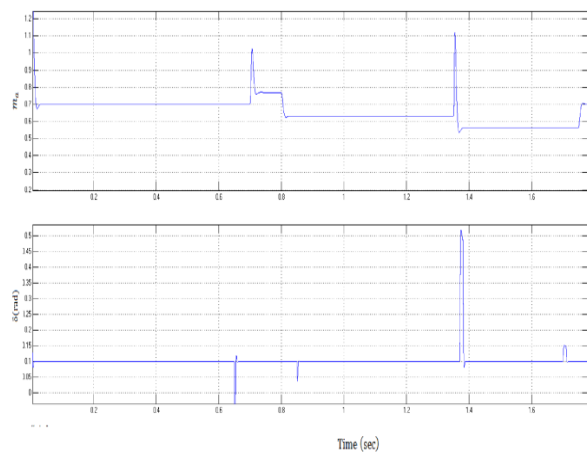


Fig-10 (b): Control inputs m_α and δ

Fig-10: Simulation results of VSC with fuzzy logic controller

The Simulation results of VSC with fuzzy logic controller design shown in Fig. 10. By observing Fig. 10 the fuzzy logic controller could produce source current closer to sinusoidal in nature this making it in phase with

the source voltage, then improving power factor of the system. The settling time of DC capacitor voltage less when compared to vector control.

6.3 Adaptive Control:

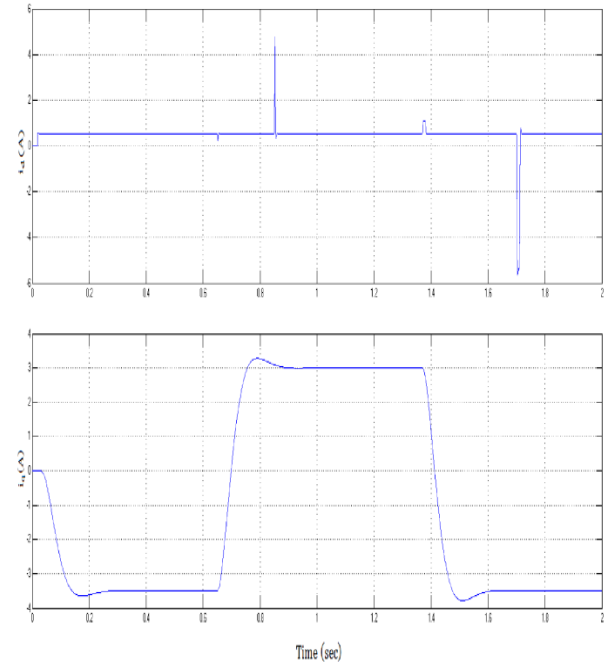
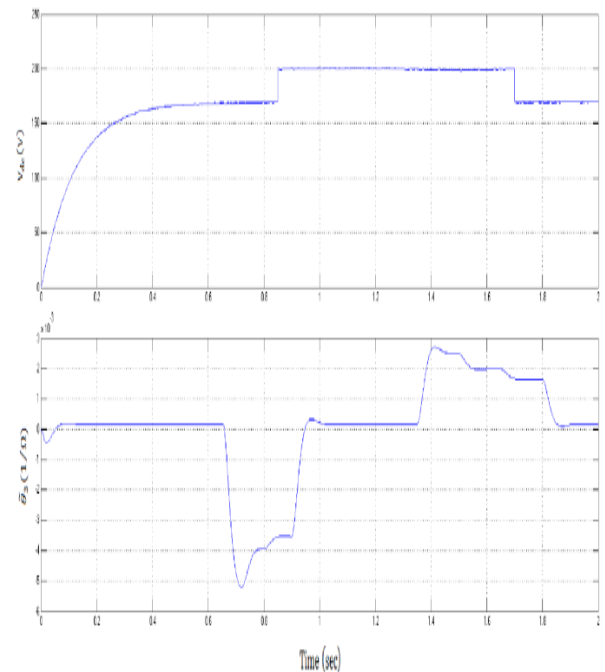


Fig-11(a): Trajectories of state and reference.



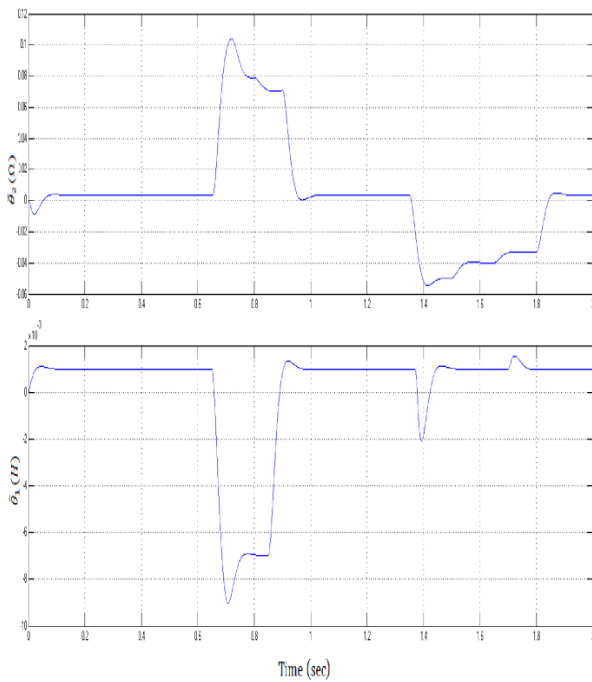


Fig-11(b): Parameter estimation error in simulation results of adaptive control using the VSC nonlinear average model.

Fig-11: Simulation Results of Adaptive Control VSC Nonlinear Average Model.

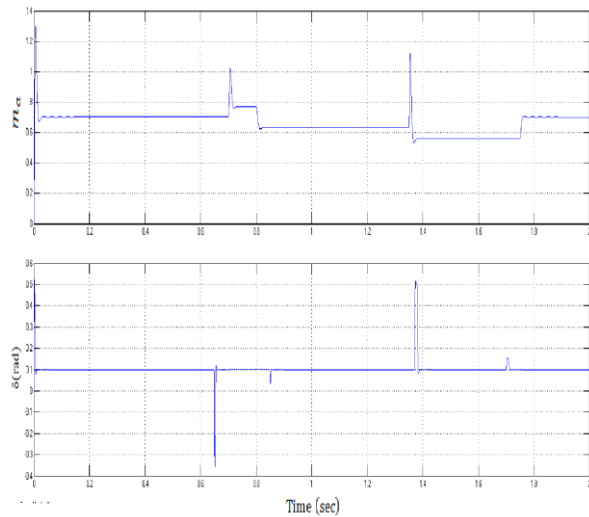
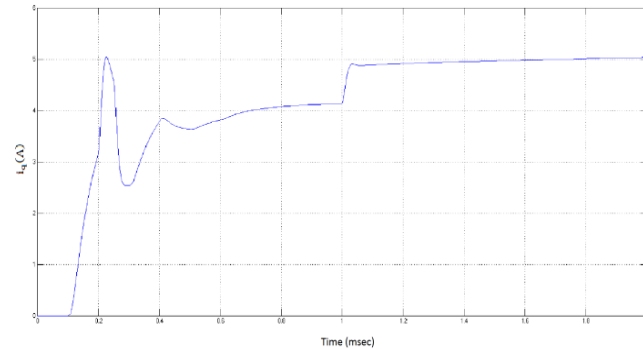


Fig-12: Simulation Results of Adaptive Control VSC Nonlinear Average Model control inputs m_a and δ

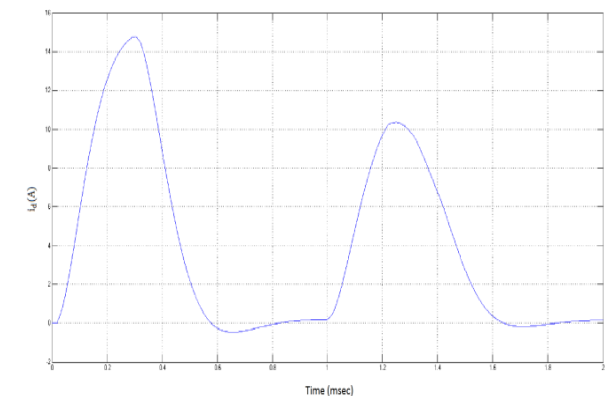
The q-axis current reference changes between $-3A$ to $3A$, and the dc voltage reference changes between 170 and $200V$. Fig. 11(a) verifies the controller's good tracking performance. The control inputs modulation index m_a and phase shift δ are depicted in Fig. 11(b). It is clear from this figure that the inputs stay within their bounds.

The parameter convergence is shown in Fig. 12 the three parameter errors converge to zero, i.e., all parameter estimates

converge to their actual values. It can be observed



that step reference changes initially affect all system variables including the system state and estimated parameters. The effect of this change is attenuated rapidly and tracking error convergence is observed. The



control gains were chosen to adjust system transient response. The dc voltage transient is indirectly controlled by d-axis current response. Hence, k_1 and k_3 were chosen sufficiently large to reduce an overshoot and increase speed of dc voltage response. It can be observed to keep control amplitudes reasonable, these gains not chosen too large.

6.4 Adaptive Control Switched VSC Model and RL Load

Fig-13: Simulation results of adaptive control using VSC nonlinear switched model with RL load: Trajectories of state, reference and control inputs m_a and δ

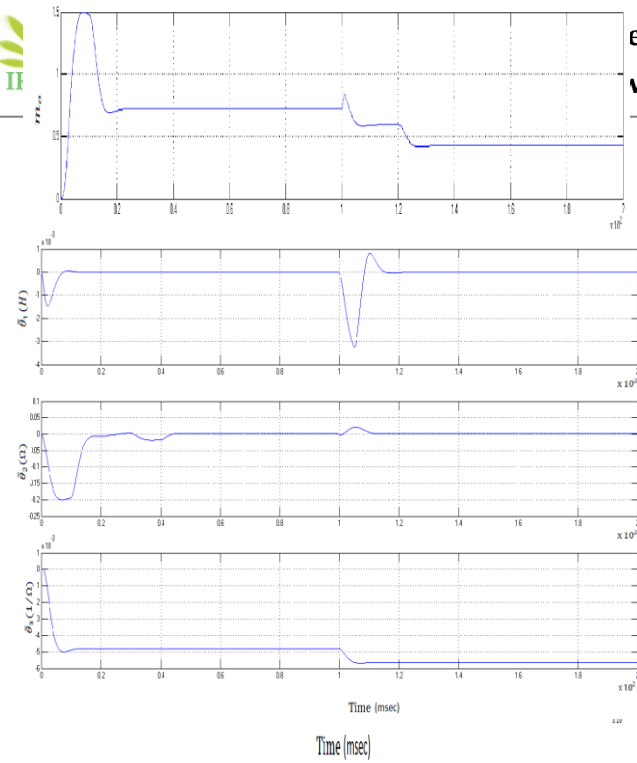
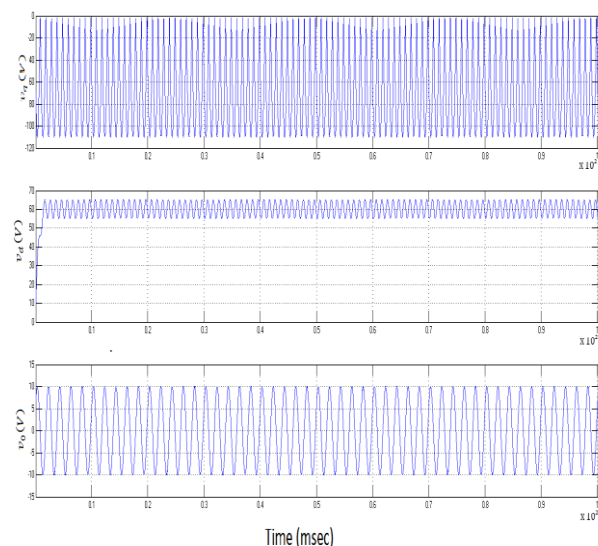


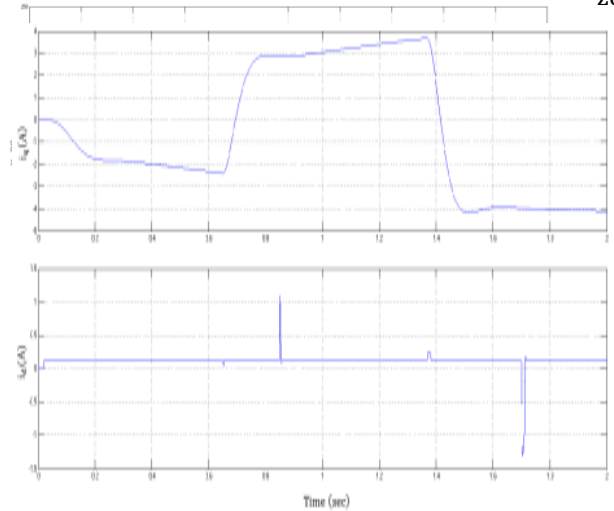
Fig-14: Simulation results of adaptive control using VSC nonlinear switched model with RL load: Parameter estimate error

A balanced three phase RL load is connected to the ac source and the load current is used to generate the q-axis current reference. The PWM carrier frequency is used $10^4 Hz$, this value is taken in simulation work. The dc voltage varies between 170 and 200V. Each phase of load consists of 12Ω resistor in parallel with inductive load $(3.6 + j\omega 0.047)\Omega$. the reference $i_{qr} = -i_{qL}$ ensures source zero q-axis current at the ac source. The simulation results are captured for 200ms, which is enough time for signal to reach steady state. Fig.6.7. demonstrates good tracking performance for i_q and v_{dc} and the control signals remain in their unsaturated ranges. The rise time for v_{dc} is less than 50ms. The parameter estimates convergence to values close to zero to compensate system uncertainty as depicted in Fig-6.8.



6.5 Adaptive Control of A Nonlinear Switched VSC Model And Imbalance Ac Source

Fig-15: Simulation results of adaptive control of a nonlinear switched VSC model and imbalance ac source: ZOO



m of ac source voltage in dqo frame

Fig-16: Simulation results of adaptive control of a nonlinear switched VSC model and imbalance ac source: Trajectories of state and reference

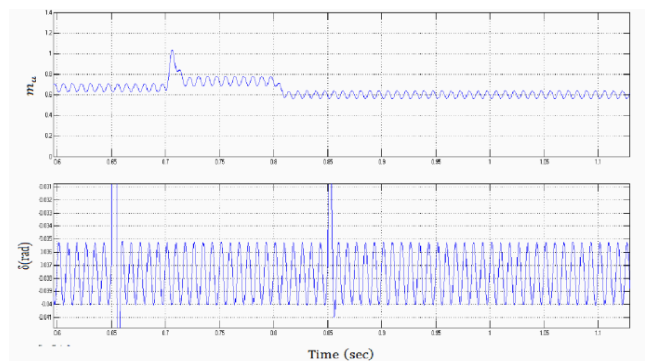


Fig-17: Simulation results of control inputs in adaptive control using a nonlinear switched VSC model and imbalance ac source

An imbalanced source is considered where phase-a of the ac source voltage is phase shifted by $\pi/8$. As shown in Fig. 15, the v_o component in the dqo frame is nonzero and also v_d and v_q has sinusoidal components with frequency twice that of the source. From Fig. 16 it is clear that the controller performs well with an imbalanced source with performance roughly as same as balanced case. In Fig. 17 we notice the control input contains sinusoidal components with frequency twice with the ac

source frequency, this effectively components for the sinusoidal changes in $v_{d,qo}$.

7. CONCLUSION

The main objective of this paper is to develop novel modelled –base control techniques For the VSC to perform PFC and harmonic elimination. This paper presented an adaptive control of a VSC used as a STATCOM for power factor correction. The method relies on a simplified model whose dc voltage dynamics assumes no resistive losses on the ac side. These losses are compensated for in directly in steady state using an effective dc side resistance. The convergence of the trajectory tracking error for the proposed model is proven. This allows for a simpler design based on an proposed VSC model but yet achieves exact trajectory tracking for the actual nonlinear model. Nonlinear average and switched models of the VSC are employed to investigate the controller performance in simulation. In particular, the simulations show the steady-state dc side resistance estimate converges to a value which compensates for model error. The performance of the adaptive control is compared with a traditional vector control and fuzzy logic control in simulation and experiment. The results confirm the simulated asymptotic stability of the tracking error, the design's robustness to un modelled effects, and the relative ease in controlling the closed-loop transient performance.

REFERENCES

- [1]. B. Singh, K. Al-Haddad, and A. Chandra, "A review of active filters for power quality improvement", IEEE Trans on Industry Applications, Vol.46, No.5, Oct 1991, pp.960-971.
- [2]. F.Z. Peng, "Application issue of active power filters", IEEE Trans on Industry Applications magazine , Vol.4, No.5, Oct 1998, pp.21-30.
- [3]. C. Schauder and H. Mehta, "Vector analysis and control of static VAR compensators", IEE Proc Generation Transmission Distribution, Vol.4, No.5, Oct 1998, pp.21-30.
- [4]. M. H. Rashid, Power Electronics Circuits , Devices and Applications, Upper saddle River, 2003,NJ: Prentice Hall.
- [5]. Rasoul M. Milasi, Alan F. Lynch and Yun Wei Li, "Adaptive Control of a Voltage Source Converter for Power Factor Correction", IEEE Transactions on Power Electronics, Vol. 28, No. 10, Oct 2013, pp. 4767-4779.
- [6]. R. H Park, "Two reaction theory of synchronous machines", IEEE Trans on American Int Electrical engineering, Vol.48, 1929, pp.716-727.
- [7]. G. Tao, "Adaptive control design and analysis", Hoboken,2003, NJ Willey.
- [8]. R. Marino and P. Tomei, "nonlinear control design and geometric, adaptive ans robust. Hertfordshire, U.K, 1995, prentice-hall.
- [9]. H. Khalil, "Nonlinear systems", Upper saddle River, 2002,NJ: Prentice Hall.
- [10]. S. Rahmani, N. Medalek and K. Al-Haddad, "Experimental design of a nonlinear control technique for three-phase shunt active power filter", IEEE Trans. Ind. Electron.,vol.57, no.10,Oct 2010, pp.3364–3375.
- [11]. A. Tabesh and R. Iravani, "multivariable dynamic model and robust control of a voltage-source converter for power system applications", IEEE Trans. Power Del., Vol.24, No.1, Jan 2009, pp.462-471.
- [12]. K. K. Shyu, M. Ji Yang, Yi Fei Lin and Yen-Mo Chen, "Model reference adaptive control design for a shunt active power filter", IEEE Trans. Ind. Elec., Vol.55, No.1, Jan 2008, pp.97-106.
- [13]. T. Jagan Mohan Rao, P. Anil Kumar and Ch. Krishna Rao, "Voltage Source converter for the Improvement of Power Quality Using Fuzzy Logic Controller", IJERA Eng. Res. And Application, Vol.4, No.5, May 2014, pp.46-50.
- [14]. V. S. C. Ravi raj and P. C. Sen, "Comparative study of Proportional-Integral, Sliding mode and fuzzy logic controllers for power converter", IEEE Trans. On industry Applications, Vol.33, No.2, April 1997, pp.97-106.
- [15]. S. K. Jain, P. Agarwal and H. O. Gupta, "fuzzy logic controlled shunt active power filter for power quality improvement", Proceedings of Institute of Electrical Engineers, Electrical power applications, Vol.149, No.5, 2002.

BIOGRAPHIES

1. V.NAVEEN,PG STUDENT, EEE Dept., JNTUA CEA, ANANTAPURA, ANDHRAPRADESH, INDIA
Mail id: v.naveen3217@gmail.com
Mobile no-9966850549
2. P. BHARAT KUMAR M. Tech (Ph.D.),LECTURER, EEE Dept., JNTUA CEA, ANANTAPUR, ANDHRAPRADESH, INDIA
Mail id: polineni3@gmail.com
Mobile no-9491389238